Developmental Cell, Vol. 3, 745–756, November, 2002, Copyright ©2002 by Cell Press

# Nodal Antagonists in the Anterior Visceral Endoderm Prevent the Formation of Multiple Primitive Streaks

**Aitana Perea-Gomez,[1,6,7] Francis D.J. Vella,[1,6] William Shawlot,[2,8] Mustapha Oulad-Abdelghani,[1] Claire Chazaud,[1,9] Chikara Meno,[3] Veronique Pfister,[1] Lan Chen,[1] Elizabeth Robertson,[4] Hiroshi Hamada,[3] Richard R. Behringer,[2] and Siew-Lan Ang[1,5,10]**

[1]IGBMC/CNRS/INSERM
Université Louis Pasteur
67404 Illkirch cedex
CU de Strasbourg
France

[2]Department of Molecular Genetics
M.D. Anderson Cancer Center
The University of Texas
Houston, Texas 77030

[3]Division of Molecular Biology
Institute for Molecular and Cellular Biology
Osaka University
Osaka 565
Japan

[4]Department of Molecular and Cellular Biology
Harvard University
Cambridge, Massachusetts 02138

## Summary

**The anterior visceral endoderm plays a pivotal role in establishing anterior-posterior polarity of the mouse embryo, but the molecular nature of the signals required remains to be determined. Here, we demonstrate that *Cerberus-like*$^{-/-}$*;Lefty1*$^{-/-}$ compound mutants can develop a primitive streak ectopically in the embryo. This defect is not rescued in chimeras containing wild-type embryonic, and *Cerberus-like*$^{-/-}$*;Lefty1*$^{-/-}$ extraembryonic, cells but is rescued in *Cerberus-like*$^{-/-}$*; Lefty1*$^{-/-}$ embryos after removal of one copy of the *Nodal* gene. Our findings provide support for a model whereby *Cerberus-like* and *Lefty1* in the anterior visceral endoderm restrict primitive streak formation to the posterior end of mouse embryos by antagonizing Nodal signaling. Both antagonists are also required for proper patterning of the primitive streak.**

## Introduction

After implantation at 5.5 dpc, the mouse egg cylinder has a proximodistal axis about which the embryo appears to be radially symmetrical. The first sign of symmetry breaking becomes morphologically apparent as epiblast cells delaminate into the primitive streak, when gastrulation begins, at 6.5 dpc The primitive streak is a transient structure formed at the posterior end of the embryo that coordinates cell movements critical for the establishment of the body plan of the amniote embryo (reviewed in Tam and Behringer, 1997). Despite the importance of this structure for embryonic patterning and morphogenesis, little is known of the molecular and cellular mechanisms that regulate the formation, location, and patterning of the primitive streak.

Insights into the molecules inducing primitive streak formation have come from embryological experiments in chick. Vg1 and Wnt8C are thought to act cooperatively in the posterior marginal zone to induce a primitive streak in chick embryos (Skromne and Stern, 2001). These genes appear to act upstream of Nodal to initiate primitive streak formation (Bertocchini and Stern, 2002 [this issue of *Developmental Cell*]). In mouse embryos, an essential role for Wnt signals has recently been demonstrated by the absence of a primitive streak in *Wnt3*$^{-/-}$ embryos (Liu et al. 1999). Misexpression of chick *Wnt8C* can also induce an additional streak in the mouse (Popperl et al., 1997). *Nodal*$^{-/-}$ mouse embryos also fail to gastrulate and lack most mesoderm, indicating an important role for *Nodal*, a TGFβ superfamily molecule, in primitive streak formation (Zhou et al., 1993; Conlon et al., 1994). In addition, *Nodal* is required in the epiblast for the specification of the anterior visceral endoderm (AVE) (Brennan et al., 2001).

Embryological experiments in mouse have provided support for an important role of the AVE in anterior patterning (Thomas and Beddington, 1996). Chimeric studies of compound *HNF3β/Foxa2* and *Lim1/Lhx1* (Perea-Gomez et al., 1999) and *Otx2* mutants (Rhinn et al., 1998; Perea-Gomez et al., 2001a) have demonstrated a role for these genes in the visceral endoderm, presumably the AVE, for inhibiting the expression of primitive streak markers in anterior epiblast. In addition explant recombination experiments have demonstrated that signals derived from the AVE can downregulate the expression of primitive streak markers in the epiblast (Kimura et al., 2000). The AVE expresses secreted molecules, including two antagonists of Nodal signaling, Cerberus-like (Cerl) and a TGFβ superfamily molecule, Lefty1 (reviewed in Perea-Gomez et al., 2001b; Sakuma et al., 2002). Mouse Cerl, a cysteine knot DAN family protein related to *Xenopus* Cerberus, can block Nodal as well as BMP signaling (Belo et al., 1997, 2000; Piccolo et al., 1999). Together, these facts led us and others to suggest that the AVE secretes antagonists, such as Cerl and Lefty1, that regulate the expression and/or activity of primitive streak inducing signals such as Nodal (Beddington and Robertson, 1999; Perea-Gomez et al., 1999, 2001a, 2001b; Kimura et al., 2000).

Given the existence of multiple Nodal antagonists, Lefty1, Cerl, and Lefty2 (Meno et al., 1999), loss-of-function studies are necessary for identifying both specific and redundant roles of these regulators in the mouse

[5]Correspondence: sang@nimr.mrc.ac.uk
[6]These authors contributed equally to this work.
[7]Present address: Institut Jacques Monod, CNRS, Universités Paris 6 et 7, 75251 Paris Cedex 05, France.
[8]Present address: Department of Genetics, Cell Biology and Development, University of Minnesota, Minneapolis, Minnesota 55455.
[9]Present address: Samuel Lunenfeld Research Institute, Mount Sinai Hospital, Toronto, Ontario M5G 1X5, Canada.
[10]Present address: Division of Developmental Neurobiology, National Institute for Medical Research, The Ridgeway, Mill Hill, London NW7 1AA, United Kingdom.

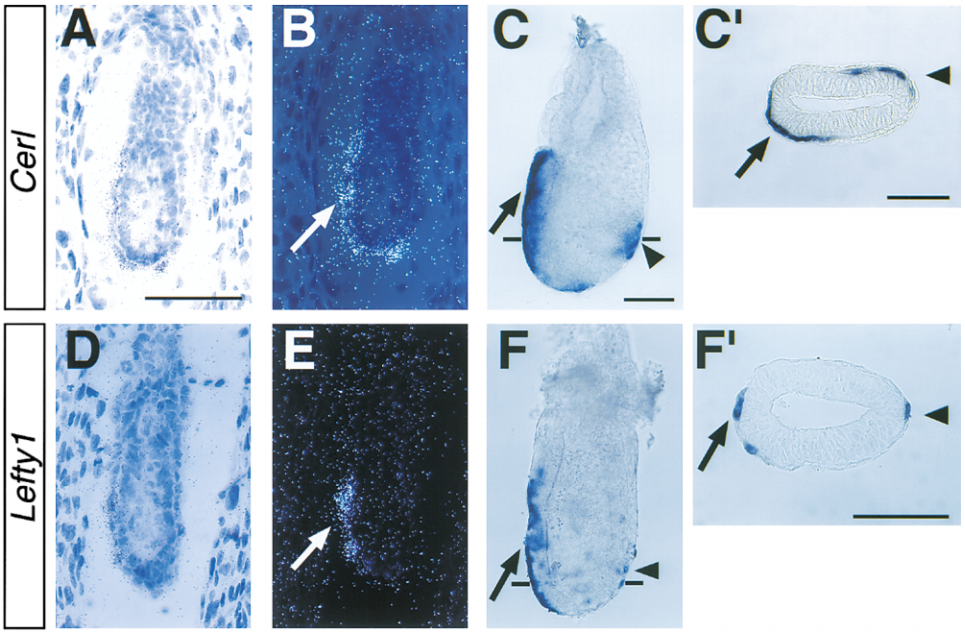


Figure 1. Overlapping Expression of *Cerl* and *Lefty1* in the AVE and ADE Precursors

(A, B, D, and E) Radioactive in situ hybridization on sagittal sections of wild-type embryos at 5.75 dpc. Brightfield (A and D) and corresponding darkfield views (B and E). Arrows indicate expression in the AVE.

(C and F) Whole-mount analysis of wild-type embryos at 7.0 dpc.

(C′ and F′) Corresponding transverse sections. Arrows indicate expression in the AVE, while arrowheads point to expression in ADE precursors derived from the APS. Magnification is the same in (A), (B), (D), and (E) and in (C) and (F). Scale bars are 100 μm.

embryo during gastrulation. *Lefty2* mutant embryos exhibit an excess of mesoderm formation, consistent with a role for Lefty2 in antagonizing Nodal signaling (Meno et al., 1999). Surprisingly, despite the potent biological activities of Lefty1 and Cerl proteins as Nodal antagonists, mice carrying null mutations in *Lefty1* (Meno et al., 1998) or *Cerl* (Simpson et al., 1999; Stanley et al., 2000; Belo et al., 2000; Shawlot et al., 2000) do not show any overt phenotype during gastrulation, possibily due to genetic redundancy (reviewed in Perea-Gomez et al., 2001b).

We therefore generated compound *Cerl* and *Lefty1* mutants and found that these embryos develop an expanded anterior primitive streak (APS) and fail to form the middle primitive streak and its derivatives. Strikingly, an ectopic primitive streak is also observed in some $Cerl^{-/-};Lefty1^{-/-}$ embryos. This phenotype is not rescued in chimeras made of wild-type embryonic tissues and $Cerl^{-/-};Lefty1^{-/-}$ extraembryonic tissues, indicating an important role for these genes in the AVE for regulating primitive streak formation. Moreover, $Cerl^{-/-};Lefty1^{-/-}$ mutant phenotypes are partially rescued in mice carrying a single copy of *Nodal*. Altogether, these findings provide support for a model whereby the AVE functions to restrict primitive streak formation posteriorly, by modulating Nodal activity through the redundant activities of Cerl and Lefty1.

## Results

### Embryonic Lethality of $Cerl^{-/-};Lefty1^{-/-}$ Mutant Embryos

*Cerl* and *Lefty1* are expressed in the AVE at 5.75 dpc prior to gastrulation until just before the late streak stage at 7.5 dpc (Figures 1A–1F; Belo et al., 1997, Oulad-Abdelghani et al., 1998). Both genes are also expressed in a few cells in the endoderm layer of the anterior primitive streak, starting at the midstreak stage at 7.0 dpc (Figures 1C, 1C′, 1F, and 1F′). Lineage studies have suggested that these cells correspond to precursors of the anterior definitive endoderm (ADE) and give rise to descendants in the foregut (Lawson and Pedersen, 1987). *Cerl*, but not *Lefty1*, transcripts are maintained in definitive endoderm cells as they migrate anteriorly and are also found in the axial mesoderm at the late streak and headfold stages (Belo et al., 1997; Oulad-Abdelghani et al., 1998, Meno et al., 1999).

To determine whether *Cerl* and *Lefty1* have redundant functions during gastrulation, we generated compound mutant embryos by crossing $Lefty1^{EIV/+}$ (see Experimental Procedures) and $Cerl^{-/-}$ (Shawlot et al., 2000) mutant mice. Since $Cerl^{-/-};Lefty1^{EIV/EIV}$ embryos show a variable phenotype at 7.5 dpc (see below), we also generated $Cerl^{-/-};Lefty1^{null/null}$ embryos (n = 15) by crossing $Lefty1^{null/+}$ (Meno et al., 1998) and $Cerl^{-/-}$. These mutants show the same variable phenotypes as the $Cerl^{-/-};Lefty1^{EIV/EIV}$ mutants, indicating that the same range of phenotypes arise in embryos completely lacking *Cerl* and *Lefty1* activity and that $Lefty^{EIV}$ is likely to be a null or severe hypomorphic allele. Supporting the latter interpretation, a fraction of $Lefty1^{EIV/EIV}$ mutants (33%) exhibited left pulmonary isomerism at 17.5 dpc and neonatal stages, as did $Lefty1^{null/null}$ embryos (Meno et al., 1998). Given the similar phenotypes, we pooled the data obtained from both genotypic classes of embryos and referred to them collectively as $Cerl^{-/-};Lefty1^{-/-}$ embryos. When $Cerl^{-/-};Lefty1^{+/-}$ mice were intercrossed, no $Cerl^{-/-};Lefty1^{-/-}$ pups were born (0 out of 92 newborns),

indicating an essential role for *Cerl* and *Lefty1* during embryonic development. Analysis of the genotypes of embryos recovered at different stages revealed that normal Mendelian ratios were recovered up to 8.5 dpc (Table 1). By 9.5 dpc, the percentage of *Cerl*$^{-/-}$;*Lefty1*$^{-/-}$ embryos was 9.4%, suggesting that these mutants start to die around this stage. Taken together, these results demonstrate that *Cerl* and *Lefty1* are required for development of the mouse embryo around the time of gastrulation and that the two genes compensate for the loss of each other.

### Variable Phenotypes of *Cerl*$^{-/-}$;*Lefty1*$^{-/-}$ Embryos

The phenotype of *Cerl*$^{-/-}$;*Lefty1*$^{-/-}$ embryos can be observed as early as 6.5 dpc. At this stage, the mutant embryos show an abnormal accumulation of visceral endoderm cells at the presumed anterior pole of the embryo, coinciding with a morphological indentation (Figures 2B and 2B′). In addition, histological sections revealed an abnormal thickening of the proximal anterior epiblast (Figure 2B′). These defects persist at 7.5 dpc (Figures 2D′, 2E″, 2F, and 2F′).

The phenotype of the *Cerl*$^{-/-}$;*Lefty1*$^{-/-}$ mutant is variable from 7.5 dpc until 9.5 dpc. We have classified the mutant embryos into three classes. Class II (42.8% of *Cerl*$^{-/-}$;*Lefty1*$^{-/-}$ mutants, n = 18) and class III embryos (28.6% of the mutants, n = 12) can be easily distinguished from class I embryos (28.6% of the mutants, n = 12) because, in these two classes, the embryonic and extraembryonic regions are separated by a tight constriction, resulting in the physical separation of embryonic and extraembryonic ectoderm (Figures 2E, 2E′, 2F, 2F′, 3C, and 3F). Previous studies of embryos mutant for *Otx2* have shown that this constriction is caused by defects in the visceral endoderm (Rhinn et al., 1998). In class III mutants, in addition, the anterior and/or lateral ectoderm protrusions contact the opposite side of the ectoderm, leading to a pinching of the embryonic region (Figures 2F and 2F′), which becomes separated into two or three distinct embryonic axes easily visualized at 8.5 dpc and 9.5 dpc (Figures 4F, 4J, 4L, and data not shown). In some cases, an accumulation of pyknotic cells arising from these ectodermal protrusions is found in the amniotic cavity of all classes of embryos (Figure 2E″ and data not shown).

All classes of mutant embryos undergo gastrulation; however, the distal tip of class I and class II mutant embryos appears thickened because of the accumulation of mesenchymal cells between the ectoderm and endoderm germ layers (Figures 2D″ and 2E′). In class III embryos, mesoderm cells are only observed in the proximal posterior region (Figure 2F″). These gastrulation defects are further analyzed with molecular markers below, first in class I and class II mutants and then in class III mutants.

### Abnormal Primitive Streak Patterning in Class I and Class II *Cerl*$^{-/-}$;*Lefty1*$^{-/-}$ Embryos

Lineage and fate map studies indicate that the primitive streak can be divided into three regions, proximal, middle, and anterior, which are distinguished by their fates (reviewed by Tam and Behringer, 1997). The APS generates axial mesendoderm, the middle streak gives rise

Table 1. Frequencies of Genotypes Among Embryos

| | *Cerl*$^{-/-}$;*Lefty1*$^{+/-}$ Intercrosses | | | *Cerl*$^{-/-}$;*Lefty1*$^{+/-}$ × *Cerl*$^{+/-}$;*Lefty1*$^{+/-}$ Intercrosses | | | |
|---|---|---|---|---|---|---|---|
| Stage | *Cerl*$^{-/-}$;*Lefty1*$^{-/-}$ | *Cerl*$^{-/-}$;*Lefty1*$^{+/-}$ | Number of Embryos | *Cerl*$^{-/-}$;*Lefty1*$^{-/-}$ | *Cerl*$^{-/-}$;*Lefty1*$^{+/-}$ | *Cerl*$^{+/-}$;*Lefty1*$^{+/-}$ | Number of Embryos |
| 6.5 dpc | 28.95% | 50.00% | 76 | 13.13% | 18.18% | 13.13% | 99 |
| 7.5 and 7.75 dpc | 26.74% | 51.16% | 256 | 13.70% | 23.39% | 8.00% | 124 |
| 8.5 dpc | 19.11% | 60.29% | 68 | 16.66% | 23.33% | 13.33% | 60 |
| 9.5 dpc | 9.37% | 75.00% | 32 | – | – | – | – |
| Expected frequencies | 25.00% | 50.00% | | 12.50% | 25.00% | 12.50% | |
| Frequencies of embryos showing abnormal phenotype | 100.00% | 9.80% | | 100.00% | 15.25% | 61.93% | |

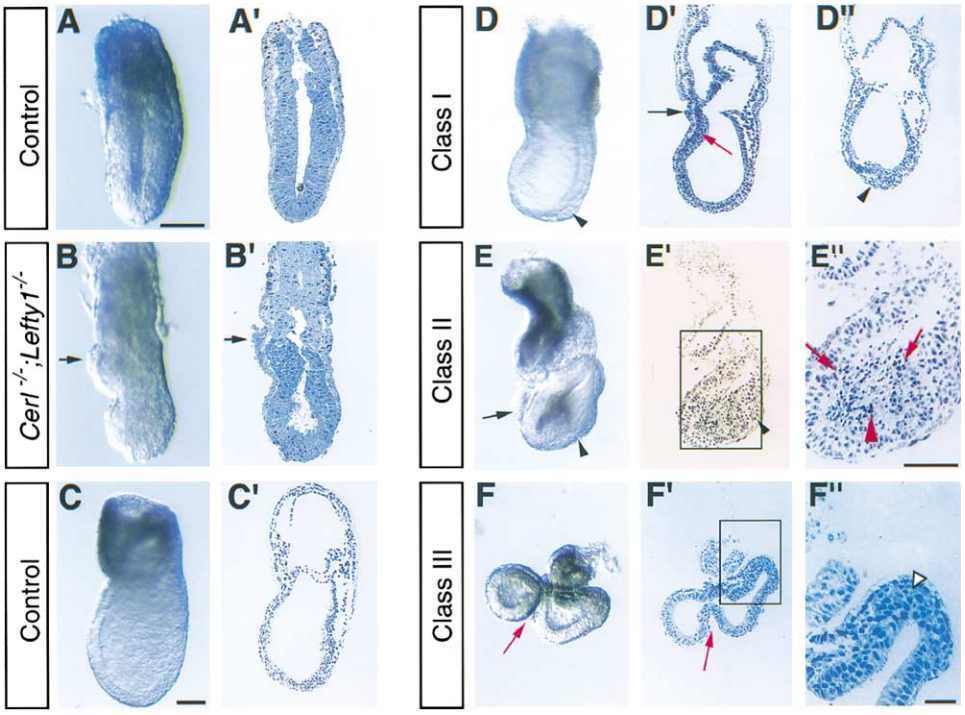


Figure 2. *Cerl*$^{-/-}$*;Lefty1*$^{-/-}$ Mutants Exhibit Defects in Visceral Endoderm and Primitive Streak Formation

(A–F and A′–F′) Morphology of wild-type embryos (A and C), *Cerl*$^{-/-}$*;Lefty1*$^{-/-}$ mutants (B and D–F), and sagittal (A′–F′) and parasagittal sections (D″) of corresponding embryos at 6.5 dpc (A–B′) and 7.5 dpc (D–F′). The abnormal accumulation of visceral endoderm cells is indicated by black arrows. Black arrowheads show an abnormal accumulation of mesenchymal cells in the distal primitive streak. An open arrowhead points to mesoderm cells. Red arrows indicate abnormalities in the ectoderm of mutant embryos. The red arrowhead points to pyknotic cells. Magnification is the same in (A)–(B′) and in (C)–(F′), except for (E″) and (F″), which are higher magnifications of the boxed region in E′ and F′, respectively. Scale bars are 100 μm in (A), (C), and (E″) and 50 μm in (F″).

to paraxial and lateral mesoderm, and descendants of the proximal streak are found extraembryonically. To further characterize *Cerl*$^{-/-}$*;Lefty1*$^{-/-}$ mutant embryos, we analyzed the expression of genes that mark different regions of the primitive streak. The T box gene *Brachyury* (*T*) is expressed in the primitive streak throughout its length, as well as in the node and axial mesendoderm at 7.5 dpc (Wilkinson et al., 1990 and Figure 3A). In class I mutants, *T* expression appeared relatively normal, as in wild-type embryos (n = 3; Figure 3B), or failed to extend as far distally in the primitive streak (n = 1; data not shown). In class II mutants (n = 2), expression of *T* in the primitive streak was severely reduced and was seen only in the proximal region of the embryo (Figure 3C; see Supplemental Figure S1A′ at http://www.developmentalcell.com/cgi/content/full/3/5/745/DC1). *T* expression was also observed in axial mesendoderm at the distal tip of class II mutants (Figure 3C; see Supplemental Figure S1A″). In contrast, we found that *Gsc* expresion, which marks the APS and axial mesendoderm at 7.5 dpc (Filosa et al., 1997 and Figure 3D), was expanded in both class I (n = 2) (Figure 3E; see Supplemental Figure S1B′) and class II mutants (n = 2) (Figure 3F; see Supplemental Figure S1C′). These results suggest an expansion of the APS and its derivative, in particular, the anteriormost axial mesendoderm expressing *Gsc*, but not *T*. Consistent with this interpretation, Foxa2 expression, another marker of the APS and all axial mesendoderm (Ang et al., 1993), is also expanded in these mutants (n = 4) (Figures 3E and 3F; see Supplemental Figures S1B′ and S1C′).

The ADE, a derivative of the APS, is also expanded in class I mutants, as shown by the expression of ADE markers, *Hex* and *SII6*. At 7.5 dpc, *Hex* expression in the ADE is enlarged laterally in class I mutants (n = 2) (Figure 3H; see Supplemental Figure S1D′), when compared with wild-types (Figure 3G; Thomas et al., 1998). Even considering a possible developmental delay of class I mutants, *Hex* expression is larger than in wild-type midstreak stage embryos (data not shown). Similarly, expression of *SII6*, a novel secreted molecule expressed in the ADE (Shimono and Behringer, 1999), was expanded in class I mutants at the same stage (n = 2; data not shown). In class II mutants at 7.5 dpc, expression of *Hex* is also expanded laterally (n = 2) (Figure 3I). However, this is most likely due to expression in the visceral endoderm because visceral endoderm cells expressing *Pem*, a marker specific for extraembryonic tissues (Lin et al., 1994), persist in the anterior embryonic region in these mutants (n = 3) (Figure 3L; see Supplemental Figure S1E′). In contrast, visceral endoderm cells are predominantly displaced into the extraembryonic region in both wild-type and class I mutant embryos (n = 2) (Figures 3J and 3K; see Supplemental Figure S1F′) by this stage.

Since the APS and its derivatives are expanded, the

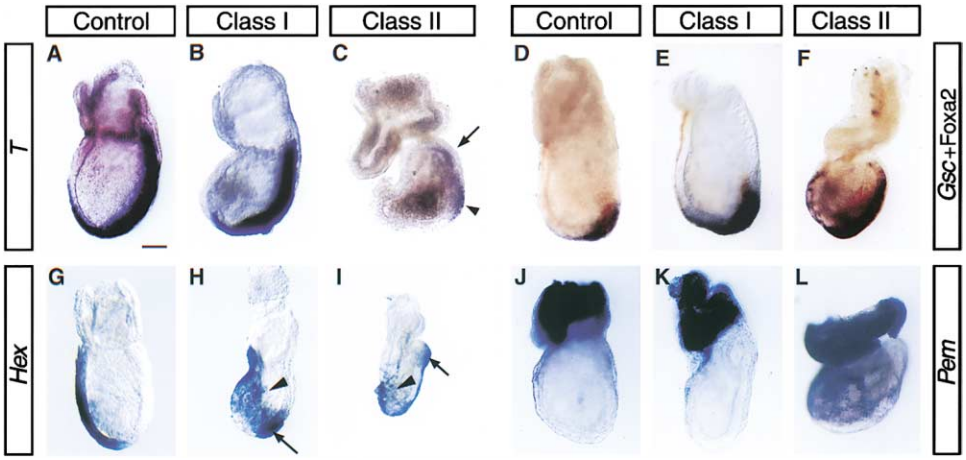


Figure 3. Abnormal Patterning of the Primitive Streak in *Cerl*$^{-/-}$;*Lefty1*$^{-/-}$ Mutants at 7.5 dpc

(A–C) Whole-mount analysis of *T* expression in control (A) and *Cerl*$^{-/-}$;*Lefty1*$^{-/-}$ (B and C) embryos. Arrowhead and arrow indicate expression in the axial mesendoderm and in the primitive streak, respectively.

(D–F) Whole-mount analysis of *Gsc* (purple) and Foxa2 (brown) expression in control (D) and *Cerl*$^{-/-}$;*Lefty1*$^{-/-}$ (E and F) embryos.

(G–I) Whole-mount analysis of *Hex* expression in control (G) and *Cerl*$^{-/-}$;*Lefty1*$^{-/-}$ (H and I) embryos. Arrowhead and arrows indicate *Hex* transcripts in the lateral regions of the embryos and at the distal tip of the primitive streak, respectively.

(J–L) Whole-mount analysis of *Pem* expression in control (J) and *Cerl*$^{-/-}$;*Lefty1*$^{-/-}$ (K and L) embryos. Magnification is the same in all panels. Scale bar is 100 μm.

status of more-proximal primitive streak regions was examined in class I and class II *Cerl*$^{-/-}$;*Lefty1*$^{-/-}$ mutants. *Tbx6* is normally expressed in nascent mesoderm cells in the middle primitive streak region, as well as in the primitive streak of wild-type embryos at 7.5 dpc (Chapman et al., 1996 and Figure 5A). At later stages, *Tbx6* is expressed in the presomitic mesoderm. In both class I and class II mutants (n = 2), no *Tbx6* transcripts were detected, indicating that paraxial mesoderm precursors are absent or misspecified (Figure 5B and data not shown). Class I and class II mutants also have severely reduced amounts of lateral mesoderm cells (data not shown). These observations, together with the abundant expression of APS and anterior axial mesendoderm markers, raise the possibility that, in class I and class II mutants, paraxial and lateral mesoderm cell populations might have been transformed into axial mesoderm. In contrast, extraembryonic mesoderm arising from more-posterior primitive streak derivatives expressing *Bmp4* (Winnier et al., 1995) and *Fgf3* (Wilkinson et al., 1989) appears relatively normal (n = 4; data not shown).

### Class III *Cerl*$^{-/-}$;*Lefty1*$^{-/-}$ Embryos Develop Multiple Primitive Streaks

In addition to an expansion of the APS and its derivatives, marked by expression of Foxa2, class III mutants at 7.75 dpc (n = 3) and 8.5 dpc (n = 3) also showed two separate sites of expression of *T* in the embryonic region, suggesting the formation of an ectopic primitive streak (Figures 4D and 4F). Foxa2 expression was also found in two sites, partially overlapping the domains of *T* expression in these embryos (Figures 4D″ and 4F′). Histological sections of whole-mount stained embryos indicated the presence of mesoderm in the two regions expressing primitive streak markers (Figures 4D′, 4D″, and 4F′). In addition, two mutant embryos that developed further than the other class III mutants showed two distinct sites of expression of an anterior neural marker, *Otx2*, as well as two domains of expression of *T* (Figure 4J), indicating the formation of ectopic axis, including the rostral brain. One class III mutant embryo was also obtained that showed three distinct sites of *T* expression (see Supplemental Figure S2B at http://www.developmentalcell.com/cgi/content/full/3/5/745/DC1). At 9.5 dpc, *Evx1* (n = 2) and *Mml* (n = 3) expression, which marks the posterior primitive streak (Dush and Martin, 1992; Pearce and Evans, 1999), are also observed in the two embryonic axes (Figure 4L and data not shown). In contrast, *Mox1* (Candia et al., 1992) transcripts were not found, suggesting the absence of paraxial mesoderm in class III mutants at 8.5 dpc and 9.5 dpc (n = 2; data not shown). Somites was also not observed in three out of four mutants at these stages (data not shown), confirming the lack of paraxial mesoderm derivatives in most cases. Altogether, these results indicate that one or two ectopic primitive streaks, expressing both anterior and posterior streak markers, and a secondary axis are formed in class III embryos.

To determine the time of formation of the ectopic primitive streak, we analyzed the expression of markers of the APS in *Cerl*$^{-/-}$;*Lefty1*$^{-/-}$ mutants at earlier stages. Since the various classes of mutants cannot be distinguished before 7.5 dpc, a random sampling of mutant embryos was analyzed. At 6.75 dpc, only a single domain of *T* (n = 3) and *Gsc* (n = 4) was observed at the posterior end of compound mutant embryos (data not shown). In contrast, one out of four *Cerl*$^{-/-}$;*Lefty1*$^{-/-}$ mutants showed ectopic expression of *T* (data not shown), and one out of five *Cerl*$^{-/-}$;*Lefty1*$^{-/-}$ mutants showed ectopic expression of *Gsc* (Figure 4B) in the anterior epiblast, at 7.25 dpc. Sections through one of these embryos revealed *Gsc* expression in two separate regions of the epiblast (Figures 4B′ and B″), one of them corresponding to an ectopic site of expression. Embryos with duplicated sites of primitive streak marker expression (n =

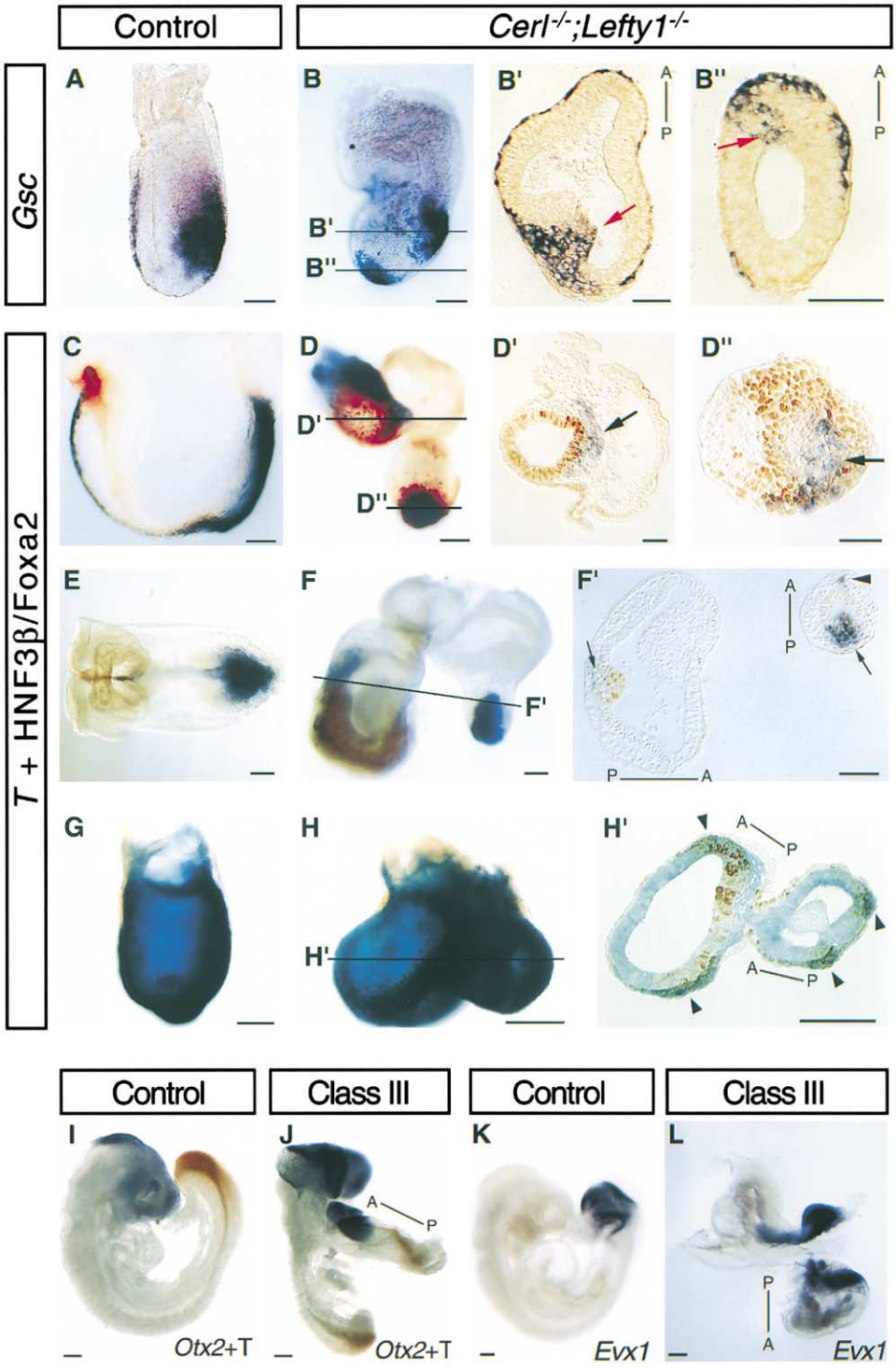


Figure 4. *Cerl* and *Lefty1* Are Required in the AVE for Preventing the Formation of Ectopic Primitive Streaks

(A and B) Whole-mount analysis of *Gsc* expression in control and *Cerl*$^{-/-}$;*Lefty1*$^{-/-}$ mutants at 7.25 dpc.

(B′and B″) Corresponding transverse sections show that *Gsc* is expressed in two distinct domains in the anterior and posterior epiblast (red arrows).

(C, D, E, and F) Whole-mount analysis of *T* (purple) and Foxa2 (brown) expression in control and class III mutants at 7.75 dpc (C and D) and 8.5 dpc (E and F).

(D′, D″, and F′) Corresponding transverse sections. Black arrows indicate nascent mesoderm expressing *T* and/or Foxa2, generated at both endogenous and ectopic primitive streaks. The black arrowhead indicates *T* and Foxa2 in a notochord-like structure in one of the embryonic halves.

(G, H, and H′) Control chimeric (G) and *Cerl*$^{-/-}$;*Lefty1*$^{-/-}$ chimeric embryos (H) at 7.75 dpc, triple-labeled for LacZ (blue), *T* (purple), and Foxa2

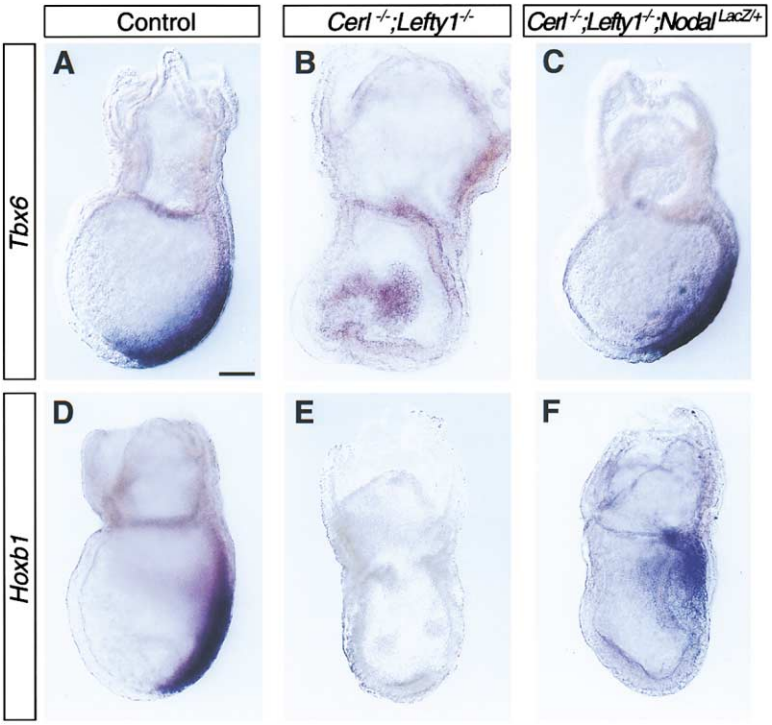


Figure 5. Rescue of Primitive Streak Patterning Defects in *Cerl*$^{-/-}$;*Lefty1*$^{-/-}$;*Nodal*$^{LacZ/+}$ Mutants at 7.5 dpc

(A–C) Whole-mount analysis of *Tbx6* expression in control (A), *Cerl*$^{-/-}$;*Lefty1*$^{-/-}$ (B), and *Cerl*$^{-/-}$;*Lefty1*$^{-/-}$;*Nodal*$^{LacZ/+}$ embryos (C).

(D–F) Whole-mount analysis of *Hoxb1* expression in control (D), *Cerl*$^{-/-}$;*Lefty1*$^{-/-}$ (E), and *Cerl*$^{-/-}$;*Lefty1*$^{-/-}$;*Nodal*$^{LacZ/+}$ embryos (F). Magnification is the same in all panels. Scale bar in (A) is 100 μm.

2) at 7.25 dpc are found at a similar frequency (22.5%, n=9) as class III mutants are found at later stages (28.6%, n = 12). Whether these embryos correspond to younger class III embryos or not, these results indicate that the earliest time of initiation of the ectopic primitive streak happens later than the endogenous streak, occurring between 6.5 dpc and 7.25 dpc, at anterior regions of the epiblast distinct from the main primitive streak. *Lefty2*, another Nodal antagonist, is still expressed in the posterior mesoderm of *Cerl*$^{-/-}$;*Lefty1*$^{-/-}$ mutants (n = 2; data not shown). Hence, the delay in ectopic primitive streak formation in these mutants may be due to the Nodal inhibitory activity of *Lefty2* that is relieved upon growth of the embryo.

In summary, class III mutants develop supernumerary primitive streaks and show the same defects in patterning of the primitive streak as do other *Cerl*$^{-/-}$;*Lefty1*$^{-/-}$ embryos.

### *Cerl* and *Lefty1* Are Required in the AVE to Regulate Primitive Streak Formation

We next determined whether *Cerl* and *Lefty1* functions are required in extraembryonic or in embryonic tissues. We generated chimeric embryos in which the embryonic tissue is more than 95% wild-type, while the extraembryonic region consists only of *Cerl*$^{-/-}$;*Lefty1*$^{-/-}$ mutant cells (Figure 4H and data not shown) by injecting wild-type *LacZ*-positive embryonic stem (ES) cells into *Cerl*$^{-/-}$;*Lefty1*$^{-/-}$ mutant morulae (Beddington and Robertson, 1989). Morphologically, these chimeras (n = 14) can be divided into three groups, corresponding to the class I, class II, and class III groups defined for *Cerl*$^{-/-}$;*Lefty1*$^{-/-}$ mutant embryos. The lack of rescue of these three phenotypic classes in these chimeras, according to morphological criteria, suggests that *Cerl* and *Lefty1* are required in extraembryonic tissues. Class III mutant chimeras were examined further for the expression of APS markers. In all three chimeras examined, *T* and Foxa2 were expressed in ectopic regions of the embryo (Figures 4H and 4H′), indicating that the presence of wild-type cells in embryonic tissues in these chimeras does not rescue the formation of ectopic primitive streaks. Together, these results show that *Cerl* and *Lefty1* are required in extraembryonic tissues, presumably the AVE, to prevent the formation of ectopic primitive streaks.

### Rescue of Primitive Streak Defects in *Cerl*$^{-/-}$;*Lefty1*$^{-/-}$ Mutant Embryos Lacking One Copy of Nodal

The defects found in *Cerl*$^{-/-}$;*Lefty1*$^{-/-}$ mutant embryos are opposite to those observed in Nodal mutants (Zhou

(brown). Corresponding transverse section (H′). Arrowheads in (H′) indicate four separate regions expressing *T*, suggesting the possibility of three ectopic primitive streaks in this chimeric embryo.

(I and J) Whole-mount analysis of *Otx2* (purple) and *T* (brown) expression in control (I) and a class III embryo (J) at 8.5 dpc with a secondary axis, including anterior neural tissues.

(K and L) Whole-mount analysis of *Evx1* expression in control (K) and class III mutants (L) at 9.5 dpc. All embryos are shown in lateral views with anterior to the left, except in (F) and where the anterior-posterior (A-P) axes are indicated. Scale bars are 100 μm, except in (B′), (B″), (D′), and (D″), where scale bars are 50 μm.

et al., 1993; Conlon et al., 1994; Brennan et al., 2001), suggesting that they may be due to an excess of Nodal signaling. To directly test this possibility, we generated *Cerl*$^{-/-}$;*Lefty1*$^{-/-}$ mutant embryos lacking one copy of the *Nodal* gene. If the defects observed in *Cerl*$^{-/-}$;*Lefty1*$^{-/-}$ mutants are caused by an excess of Nodal signaling, removal of one copy of Nodal should partially correct these defects. Mice carrying the *Nodal*$^{LacZ}$ allele (Collignon et al., 1996) were used to derive *Cerl*$^{+/-}$;*Lefty*$^{+/-}$;*Nodal*$^{LacZ/+}$ and *Cerl*$^{-/-}$;*Lefty1*$^{+/-}$;*Nodal*$^{LacZ/+}$ animals that were viable and fertile. When crossed with *Cerl*$^{-/-}$;*Lefty1*$^{+/-}$ mice, they gave rise to *Cerl*$^{-/-}$;*Lefty1*$^{-/-}$;*Nodal*$^{LacZ/+}$ embryos at the expected Mendelian frequencies, at 7.5 dpc (data not shown). At this stage, all *Cerl*$^{-/-}$;*Lefty1*$^{-/-}$;*Nodal*$^{LacZ/+}$ embryos (18/18) showed morphological defects similar to, or weaker than, those of class I *Cerl*$^{-/-}$;*Lefty1*$^{-/-}$ mutants (Figures 5C and 5F). This result suggests that elimination of one copy of *Nodal* is indeed sufficient to partially rescue the phenotype of *Cerl*$^{-/-}$;*Lefty1*$^{-/-}$ mutants, so that all compound mutant embryos belong to the milder phenotypic class. In addition, we observed that none of the *Cerl*$^{-/-}$;*Lefty1*$^{+/-}$;*Nodal*$^{LacZ/+}$ embryos analyzed (0/11) and only 12.2% (2/12) of *Cerl*$^{+/-}$;*Lefty1*$^{-/-}$;*Nodal*$^{LacZ/+}$ embryos present a mutant phenotype (of class I type) at 7.5 dpc, whereas 12.1% of *Cerl*$^{-/-}$;*Lefty1*$^{+/-}$and 61.9% of *Cerl*$^{+/-}$;*Lefty1*$^{-/-}$ mutants, respectively, exhibit class I or class II phenotypes.

To confirm the rescue of the phenotype of *Cerl*$^{-/-}$;*Lefty1*$^{-/-}$;*Nodal*$^{LacZ/+}$ compound mutants, we analyzed the expression of the paraxial mesoderm markers, *Tbx6* and *Hoxb1* (n = 3), which are not expressed in *Cerl*$^{-/-}$;*Lefty1*$^{-/-}$ mutants at 7.5 dpc (Figures 5B and 5E, respectively). In *Cerl*$^{-/-}$;*Lefty1*$^{-/-}$;*Nodal*$^{LacZ/+}$ mutants, both genes were expressed, albeit at reduced levels (n = 1 and n = 3, respectively) (Figures 5C and 5F), indicating a rescue of paraxial mesoderm formation. In addition, expression of Foxa2 in the APS appeared normal (10/12) or slightly expanded (2/12) in *Cerl*$^{-/-}$;*Lefty1*$^{-/-}$;*Nodal*$^{LacZ/+}$ mutants at 7.5 dpc and 8.5 dpc, and there were no ectopic sites of expression of Foxa2 in these embryos (12/12; data not shown).

Altogether, these results demonstrate that the primitive streak defects in *Cerl*$^{-/-}$;*Lefty1*$^{-/-}$ mutants are partially rescued after removal of one copy of the *Nodal* gene.

## Discussion

### *Cerl* and *Lefty1* Function Redundantly to Modulate Nodal Signaling during Gastrulation

Several lines of evidence indicate that *Cerl* and *Lefty1* act redundantly to inhibit Nodal signaling in the mouse gastrula. First, *Cerl*$^{-/-}$;*Lefty1*$^{-/-}$ mutants have an expanded anterior primitive streak, and a subset of them exhibit an ectopic primitive streak. These phenotypes are opposite to those of *Nodal* mutant embryos (Zhou et al., 1993; Conlon et al., 1994; Brennan et al., 2001) and have not been observed in *Cerl*$^{-/-}$ or *Lefty1*$^{-/-}$ mutants. Second, target genes of *Nodal* signaling, such as *Gsc* and *Hex*, identified in ectopic expression studies in *Xenopus* (Jones et al., 1995; Zorn et al., 1999) and zebrafish (Toyama et al., 1995; Gritsman et al., 2000), are expressed in broader domains in *Cerl*$^{-/-}$;*Lefty1*$^{-/-}$ mutants than in wild-type embryos. Third, the phenotypes of *Cerl*$^{-/-}$;*Lefty1*$^{-/-}$ mutants are partially suppressed by heterozygosity of *Nodal*. Together with other reports indicating that Cerl and antivin/Lefty act as negative feedback regulators of Nodal signaling (reviewed in Schier and Shen, 2000; Whitman, 2001), our findings demonstrate that these gene products function redundantly downstream of Nodal to attenuate its signaling activity during gastrulation.

Why are *Cerl* and *Lefty1* required to limit Nodal signaling? Perhaps more than one antagonist is required to attenuate variations in signaling levels resulting from biological noise in regulatory networks (Becksel and Serrano, 2000). It is noteworthy that previous studies have suggested that mouse embryos are very sensitive to actual levels of Nodal signaling, as the phenotypes of *Nodal* hypormorphs (Lowe et al., 2001) and *Nodal* pathway mutants, such as Fast1 (Hoodless et al., 2001; Yamamoto et al., 2001), are highly variable. We therefore propose that the variability of *Cerl*$^{-/-}$;*Lefty1*$^{-/-}$ phenotypes could be due to stochastic fluctuations in the levels of Nodal signaling in mutant embryos. Alternatively, this variability could be due to the heterogenous 129/SvxCD1 genetic background of the mutant embryos.

### *Cerl* and *Lefty1* Regulate Patterning of the Primitive Streak

In *Cerl*$^{-/-}$;*Lefty1*$^{-/-}$ mutants, there is an expansion of the APS, while the middle streak and its derivative, the paraxial mesoderm, are not generated. These defects are partially rescued by reducing Nodal dosage in compound mutants. These results indicate that the level and/or range of Nodal signaling must be tightly regulated for proper patterning of the primitive streak. The idea that Nodal may function as a morphogen in mesendoderm induction and patterning was initially supported by gain-of-function studies in *Xenopus* (Jones et al., 1995; Agius et al., 2000). Recently, studies in zebrafish embryos have provided evidence that a Nodal-related protein could function as a morphogen, inducing *Gsc* at high doses and *T* at lower doses (Chen and Schier, 2001). At early gastrulation stages in mouse embryos, *Gsc* is expressed at the anteriormost part of the primitive streak, and *T* is expressed in the rest of the primitive streak (our unpublished results). It is tempting to speculate that this molecular heterogeneity of the primitive streak is a consequence of graded levels of Nodal signaling. The specific loss of the APS in embryos carrying a null mutation in *Arkadia*, a ring finger gene modulating Nodal signaling, supports the idea that the APS requires higher levels of Nodal signaling than the rest of the primitive streak (Episkopou et al., 2001).

It may seem paradoxical that *Cerl* and *Lefty1* are expressed in ADE precursor cells directly underlying the APS, although this tissue requires high levels of Nodal signaling for the induction of genes such as *Gsc*. However, expression of *Cerl* and *Lefty1* in the ADE precursor cells is initiated only at the middle primitive streak stage, after the APS has formed and after the initiation of *Gsc* expression. This temporal delay in the activation of *Cerl* and *Lefty1* may have a role in modulating the level of Nodal signaling over time. In this way, genes such as

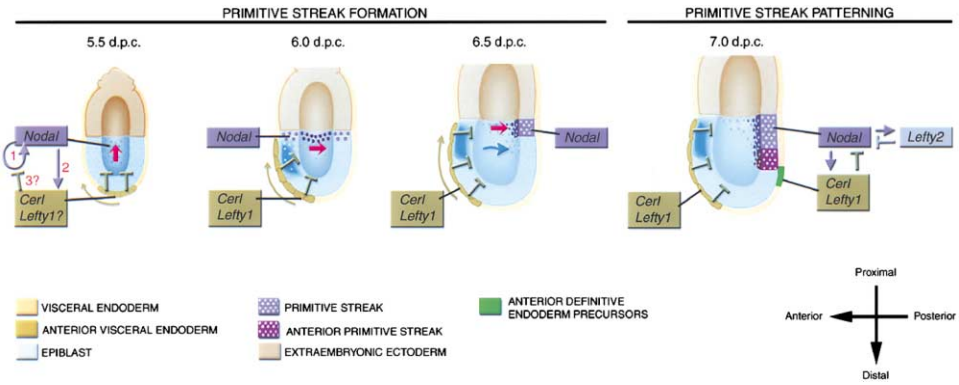


Figure 6. A Model Showing How *Cerl* and *Lefty* Genes Regulate Primitive Streak Formation and Patterning in Mouse

At 5.5 dpc, Nodal from the epiblast regulates its own expression through an autoregulatory loop (1) and the expression of genes in the AVE, including *Cerl* and *Lefty1* (2) (Brennan et al., 2001). Cerl and Lefty1 from the AVE then feed back to downregulate Nodal expression first in the distal and then in the anterior epiblast after anterior displacement of the visceral endoderm (green arrows), perhaps by inhibiting the *Nodal* autoregulatory loop (3?). As a consequence of these AVE-epiblast interactions, *Nodal* expression becomes spatially restricted, resulting in primitive streak formation at the posterior end of the embryo. The progressive spatial restriction of Nodal expression is indicated by red arrows. Migration of anterior proximal epibast cells (blue arrow) may also contribute to the restriction of Nodal signaling posteriorly. *Nodal* has also been shown to regulate the expression of genes, such as *BMP4* and *Eomesodermin*, in the extraembryonic ectoderm (Brennan et al., 2001; data not shown). At 7.0 dpc (midstreak stage), *Cerl* and *Lefty1* from the precursors of the ADE and possibly *Lefty2* from the mesoderm wings pattern the anterior-posterior axis of the streak, which will give rise to corresponding medial-lateral mesoderm populations. This figure is adapted from Beddington and Robertson (1999).

*Gsc* could be activated transiently in the APS at the early streak stage, and a different set of genes, including *chordin* (Bachiller et al., 2000) and *T*, could be expressed in the APS at later stages. Analysis of the regulatory elements of these different Nodal-induced genes may provide further insight into this problem.

### The AVE Positions the Primitive Streak by the Inhibitory Activities of Cerl and Lefty1 on Nodal Signaling

We have observed the formation of an ectopic primitive streak in all class III mutant embryos. This phenotype is rescued in *Cerl*$^{-/-}$;*Lefty1*$^{-/-}$ mutants with only one copy of the Nodal gene. In addition, the ectopic primitive streak in class III mutants is not rescued in chimeras made of wild-type embryonic tissues and *Cerl*$^{-/-}$; *Lefty1*$^{-/-}$ extraembryonic tissues, demonstrating that these genes act in the AVE to prevent multiple primitive streaks from forming in the embryo. These findings support a model whereby the AVE functions, by the inhibitory activities of *Cerl* and *Lefty1,* to restrict Nodal signaling and, consequently, primitive streak formation to the posterior end of the embryo (Figure 6). One possible explanation for the progressive posterior restriction of Nodal signaling before gastrulation could be the inhibition of its autoregulatory loop (Brennan et al., 2001) in other regions of the epiblast. Alternatively, posteriorward movement by epiblast cells could contribute to the restriction of primitive streak signals (Beddington and Robertson, 1999). Wnt signaling is also likely to play a role in primitive streak formation, given the lack of formation of a primitive streak in *Wnt3* mouse mutants (Liu et al., 1999). However, whether *Wnt3* acts in the same pathway as Nodal or independently remains to be determined.

In the mouse embryo, the future AVE cells are located in a distal position shortly after implantation and are displaced asymmetrically toward the prospective anterior side of the embryo before the onset of gastrulation (Thomas et al., 1998). Evidence for an early role of AVE precursors in regulating primitive streak formation has come from explant culture experiments (Kimura et al., 2000). These studies have also shown that signals derived from the AVE can downregulate the expression of primitive streak markers in the epiblast (Kimura et al., 2000). Since *Cerl* is already expressed in AVE precursor cells distally, as shown by the expression of a *LacZ* gene inserted into the *Cerl* locus (Stanley et al., 2000), we propose that inhibition of Nodal signaling starts distally and shifts anteriorly as a consequence of AVE cell movements (Figure 6). An important remaining question is, what drives asymmetric migration of the AVE cells?

The model shown in Figure 6 is in agreement with the finding that the hypoblast, the presumed avian equivalent of the AVE, inhibits primitive streak formation through the action of Nodal antagonists such as Cerberus (Bertocchini and Stern, 2002). In the chick embryo, the hypoblast is displaced away from the site of primitive streak formation by the endoblast, the presumed avian equivalent of posterior visceral endoderm, just before the appearance of the primitive streak. This mechanism would ensure that a single primitive streak forms above the endoblast, in the posterior epiblast (Bertocchini and Stern, 2002).

Evidence for a role of Nodal inhibitory signals in regulating primitive streak formation has also been obtained, from the phenotypic analysis of *Lefty2* mutants, which develop an enlarged primitive streak and have an excess of mesoderm (Meno et al., 1999). These data suggest that different antagonists of Nodal signaling, Cerl and Lefty1 in the AVE and Lefty2 in mesoderm cells invaginating and delaminating from the middle and posterior primitive streak, may work together to correctly position the primitive streak at the posterior end of the embryo

and/or regulate its width. Lefty2 from the mesoderm wings may also cooperate with Cerl and Lefty1 from the ADE precursors to regulate patterning of the primitive streak at the midstreak stage (Figure 6).

In conclusion, our analysis of *Cerl*$^{-/-}$*;Lefty1*$^{-/-}$ compound mutants indicates that *Cerl* and *Lefty1* function redundantly to regulate the formation and patterning of the primitive streak. Our findings provide support for a model whereby a critical step in primitive streak formation is the progressive restriction of Nodal activity to the posterior end of the embryo by the AVE-derived signals, Cerl and Lefty1. This important role of the AVE in preventing the formation of multiple primitive streaks or axes is evolutionarily conserved in the hypoblast of the chick (Bertocchini and Stern, 2002).

## Experimental procedures

### Generation of *Lefty1*$^{EIV}$ Mutant Mice

Mouse *Lefty1* genomic DNA was obtained by screening, with a mouse *Lefty1* cDNA probe, a mouse genomic library prepared from D3-ES cells (Oulad-Abdelghani et al., 1998). *The Lefty1* gene contains four exonic sequences (Oulad-Abdelghani et al., 1998), EI (338 bp), EII (247 bp), EIII (246 bp), and EIV (789 bp), encoding amino acids 1–84, 85–166, 167–248, and 249–368, respectively. The targeting strategy was designed to disrupt the mature protein, which is encoded entirely by exon EIV. Details of the targeting construct and the strategy used to analyze the ES cell lines are available from the authors upon request.

### Generation and Genotyping of *Cerl*$^{-/-}$*;Lefty1*$^{-/-}$ and *Cer;Lefty1;Nodal* Compound Mutant Mice and Embryos

All mutant mouse lines were maintained on a 129/SvxCD1 background. For the genotyping of pups and embryos, DNA was extracted from tails tips, as described (Laird et al., 1991), and from yolk sac, as described (Perea-Gomez et al., 1999).

PCR at the *Cerl* and *Lefty1* loci was performed with standard PCR conditions and the following primers. Wild-type *Cerl* allele (800 bp), forward primer 5′-CCTGCTGACCACCTGCTTCC-3′ and reverse primer 5′-GGCCACGTCCCACAATGAAT-3′; mutant *Cerl* allele (520 bp), forward primer 5′-GCCCAGAGGACTTGGTGTTG-3′ and reverse primer 5′-GACAAAGCGGTTTGAGGGGC-3′; wild-type *Lefty1* allele (280 bp), forward primer (P3) 5′-TAATAAGCTACACACCCAGC-3′ and reverse primer (P4) 5′-CTGCCCACACATTCATATGTC-3′; mutant *Lefty1*$^{EIV}$ allele (500 bp), forward primer (P1) 5′-CCCGTGATATT GCTGAAGAGCTTGG-3′ and reverse primer (P5) 5′-CTCCCAGTA TAATGAGCACTTC-3′.

Mutant *Lefty1*$^{null}$ allele and *Nodal*$^{LacZ}$ allele were genotyped as previously described (Meno et al., 1998, and Collignon et al., 1996, respectively).

### In Situ Hybridization, Immunohistochemistry, and Histology

Mouse embryos were staged according to their morphology (Downs and Davies, 1993). Whole-mount in situ hybridization was performed as described previously (Conlon and Herrmann, 1993). The number of specimens used for in situ hybridization of each gene is indicated in the results section as n = x. For section in situ hybridization, decidua were fixed for two hours in 4% paraformaldehyde in PBS, equilibrated in 20% sucrose overnight, and embedded in OCT (Tissue-Tek, Miles). In situ hybridization on 8 μm frozen sections was performed as described (Perea-Gomez et al., 1999), and sections were counterstained with hematoxylin.

For immunohistochemistry with the Foxa2 antibody after whole-mount in situ hybridization, embryos were processed as described in Filosa et al. (1997). For histological analysis, embryos were fixed in 2.5% glutaraldehyde in PBS overnight, dehydrated, and embedded in epon. Two-micrometer sections were counterstained with 1% toluidine blue.

Embryos previously processed for whole-mount in situ hybridization, were postfixed overnight in 2.5% glutaraldehyde in PBS, rinsed in PBS, and embedded with the JB-4 Embedding Kit (Polysciences). Five-micrometer sections were mounted directly.

### Generation of Chimeric Embryos

The morulae stage (2.5 dpc) embryos used to generate chimeras were obtained from intercrosses of *Cerl*$^{-/-}$*;Lefty1*$^{+/-}$ mice. Embryos were injected with approximately ten wild-type ROSA26/+ ES cells of the ES31 line (Rhinn et al., 1998) and reimplanted into pseudopregnant females. Chimeric embryos were harvested at 7.5 dpc and processed for β-galactosidase staining, and then whole-mount in situ hybridization was performed as described in Rhinn et al. (1998). The genotype of the host morula was determined retrospectively with visceral yolk sac endoderm isolated from visceral mesoderm after digestion in pancreatin and trypsin as described (Hogan et al., 1994). DNA samples from the endodermal fraction were genotyped for the *Lefty1* locus.

### Acknowledgments

We are grateful to Drs. R. Beddington, M. Blum, R. Harvey, B. Herrmann, B.L. Hogan, R. Krumlauf, K. Mahon, C. Niehrs, V.E. Papaioannou, and D.G. Wilkinson for gifts of probes, to Hiroshi Sasaki for the anti-Foxa2 antibody, to Anne Gansmuller and Mireille Digelmann for making histological sections, to Bertrand Vernay and Muriel Koch for help with experiments, and to Andrée Dierich and Marianne Lemeur for generating ES-morula chimeras. We thank members of the lab, Anne Camus, François Guillemot, Marc Hallonet, and Claudio Stern for helpful comments on the manuscript. We also thank Federica Bertocchini and Claudio Stern for sharing their unpublished data. This work was supported by grants from the Human Frontier Science Program, the European Community Biotech Programme, and the Association pour la Recherche sur le Cancer (ARC) to S.L.A. and by funds from the INSERM, the CNRS, and the Hôpital Universitaire de Strasbourg. A.P.G. and F.D.J.V. were supported by predoctoral fellowships from the Ministère de la Recherche and from ARC.

Received: March 1, 2002
Revised: September 3, 2002

### References

Agius, E., Oelgeschlager, M., Wessely, O., Kemp, C., and De Robertis, E.M. (2000). Endodermal Nodal-related signals and mesoderm induction in *Xenopus*. Development *127*, 1173–1183.

Ang, S.L., Wierda, A., Wong, D., Stevens, K.A., Cascio, S., Rossant, J., and Zaret, K.S. (1993). The formation and maintenance of the definitive endoderm lineage in the mouse: involvement of HNF3/forkhead proteins. Development *119*, 1301–1315.

Bachiller, D., Klingensmith, J., Kemp, C., Belo, J.A., Anderson, R.M., May, S.R., McMahon, J.A., McMahon, A.P., Harland, R.M., Rossant, J., and De Robertis, E.M. (2000). The organizer factors Chordin and Noggin are required for mouse forebrain development. Nature *403*, 658–661.

Becksel, A., and Serrano, L. (2000). Engineering stability in gene networks by autoregulation. Nature *405*, 590–593.

Beddington, R.S., and Robertson, E.J. (1989). An assessment of the developmental potential of embryonic stem cells in the midgestation mouse embryo. Development *105*, 733–737.

Beddington, R.S., and Robertson, E.J. (1999). Axis development and early asymmetry in mammals. Cell *96*, 195–209.

Belo, J.A., Bouwmeester, T., Leyns, L., Kertesz, N., Gallo, M., Follettie, M., and De Robertis, E.M. (1997). Cerberus-like is a secreted factor with neutralizing activity expressed in the anterior primitive endoderm of the mouse gastrula. Mech. Dev. *68*, 45–57.

Belo, J.A., Bachiller, D., Agius, E., Kemp, C., Borges, A.C., Marques, S., Piccolo, S., and De Robertis, E.M. (2000). Cerberus-like is a secreted BMP and nodal antagonist not essential for mouse development. Genesis *26*, 265–270.

Bertocchini, F., and Stern, C.D. (2002). The hypoblast of the chick embryo positions the primitive streak by antagonizing Nodal signaling. Dev. Cell *3*, this issue, 735–744.

Brennan, J., Lu, C.C., Norris, D.P., Rodriguez, T.A., Beddington, R.S., and Robertson, E.J. (2001). Nodal signalling in the epiblast patterns the early mouse embryo. Nature *411*, 965–969.

Candia, A.F., Hu, J., Crosby, J., Lalley, P.A., Noden, D., Nadeau, J.H., and Wright, C.V. (1992). Mox-1 and Mox-2 define a novel homeobox gene subfamily and are differentially expressed during early mesodermal patterning in mouse embryos. Development *116*, 1123–1136.

Chapman, D.L., Agulnik, I., Hancock, S., Silver, L.M., and Papaioannou, V.E. (1996). Tbx6, a mouse T-Box gene implicated in paraxial mesoderm formation at gastrulation. Dev. Biol. *180*, 534–542.

Chen, Y., and Schier, A.F. (2001). The zebrafish Nodal signal Squint functions as a morphogen. Nature *411*, 607–610.

Collignon, J., Varlet, I., and Robertson, E.J. (1996). Relationship between asymmetric nodal expression and the direction of embryonic turning. Nature *381*, 155–158.

Conlon, F.L., Lyons, K.M., Takaesu, N., Barth, K.S., Kispert, A., Herrmann, B., and Robertson, E.J. (1994). A primary requirement for nodal in the formation and maintenance of the primitive streak in the mouse. Development *120*, 1919–1928.

Conlon, R.A., and Herrmann, B.G. (1993). Detection of messenger RNA by in situ hybridization to postimplantation embryo whole mounts. Methods Enzymol. *225*, 373–383.

Dush, M.K., and Martin, G.R. (1992). Analysis of mouse Evx genes: Evx-1 displays graded expression in the primitive streak. Dev. Biol. *151*, 273–287.

Downs, K.M., and Davies, T. (1993). Staging of gastrulating mouse embryos by morphological landmarks in the dissecting microscope. Development *118*, 1255–1266.

Episkopou, V., Arkell, R., Timmons, P.M., Walsh, J.J., Andrew, R.L., and Swan, D. (2001). Induction of the mammalian node requires Arkadia function in the extraembryonic lineages. Nature *410*, 825–830.

Filosa, S., Rivera-Perez, J.A., Gomez, A.P., Gansmuller, A., Sasaki, H., Behringer, R.R., and Ang, S.L. (1997). Goosecoid and HNF-3beta genetically interact to regulate neural tube patterning during mouse embryogenesis. Development *124*, 2843–2854.

Gritsman, K., Talbot, W.S., and Schier, A.F. (2000). Nodal signalling patterns the organizer. Development *127*, 921–932.

Hogan, B., Beddington, R., Constantini, F., and Lacy, E. (1994). Manipulating the Mouse Embryo: A Laboratory Manual (Cold Spring Harbor, New York: Cold Spring Harbor Laboratory Press).

Hoodless, P.A., Pye, M., Chazaud, C., Labbe, E., Attisano, L., Rossant, J., and Wrana, J.L. (2001). FoxH1 (Fast) functions to specify the anterior primitive streak in the mouse. Genes Dev. *15*, 1257–1271.

Jones, C.M., Kuehn, M.R., Hogan, B.L., Smith, J.C., and Wright, C.V. (1995). Nodal-related signals induce axial mesoderm and dorsalize mesoderm during gastrulation. Development *121*, 3651–3662.

Kimura, C., Yoshinaga, K., Tian, E., Suzuki, M., Aizawa, S., and Matsuo, I. (2000). Visceral endoderm mediates forebrain development by suppressing posteriorizing signals. Dev. Biol. *225*, 304–321.

Laird, P.W., Zijderveld, A., Linders, K., Rudnicki, M.A., Jaenisch, R., and Berns, A. (1991). Simplified mammalian DNA isolation procedure. Nucleic Acids Res. *19*, 4293.

Lawson, K.A., and Pedersen, R.A. (1987). Cell fate, morphogenetic movement and population kinetics of embryonic endoderm at the time of germ layer formation in the mouse. Development *101*, 627–652.

Lin, T.P., Labosky, P.A., Grabel, L.B., Kozak, C.A., Pitman, J.L., Kleeman, J., and MacLeod, C.L. (1994). The Pem homeobox gene is X-linked and exclusively expressed in extraembryonic tissues during early murine development. Dev. Biol. *166*, 170–179.

Liu, P., Wakamiya, M., Shea, M.J., Albrecht, U., Behringer, R.R., and Bradley, A. (1999). Requirement for Wnt3 in vertebrate axis formation. Nat. Genet. *22*, 361–365.

Lowe, L.A., Yamada, S., and Kuehn, M.R. (2001). Genetic dissection of nodal function in patterning the mouse embryo. Development *128*, 1831–1843.

Meno, C., Shimono, A., Saijoh, Y., Yashiro, K., Mochida, K., Ohishi, S., Noji, S., Kondoh, H., and Hamada, H. (1998). lefty-1 is required for left-right determination as a regulator of lefty-2 and nodal. Cell *94*, 287–297.

Meno, C., Gritsman, K., Ohishi, S., Ohfuji, Y., Heckscher, E., Mochida, K., Shimono, A., Kondoh, H., Talbot, W.S., Robertson, E.J., et al. (1999). Mouse Lefty2 and zebrafish antivin are feedback inhibitors of nodal signalling during vertebrate gastrulation. Mol. Cell *4*, 287–298.

Oulad-Abdelghani, M., Chazaud, C., Bouillet, P., Mattei, M.G., Dolle, P., and Chambon, P. (1998). Stra3/lefty, a retinoic acid-inducible novel member of the transforming growth factor-beta superfamily. Int. J. Dev. Biol. *42*, 23–32.

Pearce, J.J., and Evans, M.J. (1999). Mml, a mouse Mix-like gene expressed in the primitive streak. Mech. Dev. *87*, 189–192.

Perea-Gomez, A., Shawlot, W., Sasaki, H., Behringer, R.R., and Ang, S. (1999). HNF3beta and Lim1 interact in the visceral endoderm to regulate primitive streak formation and anterior-posterior polarity in the mouse embryo. Development *126*, 4499–4511.

Perea-Gomez, A., Lawson, K.A., Rhinn, M., Zakin, L., Brulet, P., Mazan, S., and Ang, S.L. (2001a). Otx2 is required for visceral endoderm movement and for the restriction of posterior signals in the epiblast of the mouse embryo. Development *128*, 753–765.

Perea-Gomez, A., Rhinn, M., and Ang, S.L. (2001b). Role of the anterior visceral endoderm in restricting posterior signals in the mouse embryo. Int. J. Dev. Biol. *45*, 311–320.

Piccolo, S., Agius, E., Leyns, L., Bhattacharyya, S., Grunz, H., Bouwmeester, T., and De Robertis, E.M. (1999). The head inducer Cerberus is a multifunctional antagonist of Nodal, BMP and Wnt signals. Nature *397*, 707–710.

Popperl, H., Schmidt, C., Wilson, V., Hume, C.R., Dodd, J., Krumlauf, R., and Beddington, R.S. (1997). Misexpression of Cwnt8C in the mouse induces an ectopic embryonic axis and causes a truncation of the anterior neuroectoderm. Development *124*, 2997–3005.

Rhinn, M., Dierich, A., Shawlot, W., Behringer, R.R., Le Meur, M., and Ang, S.L. (1998). Sequential roles for Otx2 in visceral endoderm and neuroectoderm for forebrain and midbrain induction and specification. Development *125*, 845–856.

Sakuma, R., Ohnishi, Y.Y., Meno, C., Fujii, H., Juan, H., Takeuchi, J., Ogura, T., Li, E., Miyazono, K., and Hamada, H. (2002). Inhibition of Nodal signalling by Lefty mediated through interaction with common receptors and efficient diffusion. Genes Cells *7*, 401–412.

Schier, A.F., and Shen, M.M. (2000). Nodal signalling in vertebrate development. Nature *403*, 385–389.

Shawlot, W., Min Deng, J., Wakamiya, M., and Behringer, R.R. (2000). The cerberus-related gene, Cerr1, is not essential for mouse head formation. Genesis *26*, 253–258.

Shimono, A., and Behringer, R.R. (1999). Isolation of novel cDNAs by subtractions between the anterior mesendoderm of single mouse gastrula stage embryos. Dev. Biol. *209*, 369–380.

Simpson, E.H., Johnson, D.K., Hunsicker, P., Suffolk, R., Jordan, S.A., and Jackson, I.J. (1999). The mouse Cer1 (Cerberus related or homologue) gene is not required for anterior pattern formation. Dev. Biol. *213*, 202–206.

Skromne, I., and Stern, C.D. (2001). Interactions between Wnt and Vg1 signalling pathways initiate primitive streak formation in the chick embryo. Development *128*, 2915–2927.

Stanley, E.G., Biben, C., Allison, J., Hartley, L., Wicks, I.P., Campbell, I.K., McKinley, M., Barnett, L., Koentgen, F., Robb, L., and Harvey, R.P. (2000). Targeted insertion of a LacZ reporter gene into the mouse Cer1 locus reveals complex and dynamic expression during embryogenesis. Genesis *26*, 259–264.

Tam, P.P., and Behringer, R.R. (1997). Mouse gastrulation: the formation of a mammalian body plan. Mech. Dev. *68*, 3–25.

Thomas, P., and Beddington, R. (1996). Anterior primitive endoderm may be responsible for patterning the anterior neural plate in the mouse embryo. Curr. Biol. *6*, 1487–1496.

Thomas, P.Q., Brown, A., and Beddington, R.S. (1998). Hex: a homeobox gene revealing peri-implantation asymmetry in the mouse

embryo and an early transient marker of endothelial cell precursors. Development *125*, 85–94.

Toyama, R., O'Connell, M.L., Wright, C.V., Kuehn, M.R., and Dawid, I.B. (1995). Nodal induces ectopic *goosecoid* and *Lhx1* expression and axis duplication in zebrafish. Development *121*, 383–391.

Whitman, M. (2001). Nodal signaling in early vertebrate embryos: themes and variations. Dev. Cell *1*, 605–617.

Wilkinson, D.G., Bhatt, S., and Herrmann, B.G. (1990). Expression pattern of the mouse T gene and its role in mesoderm formation. Nature *343*, 657–659.

Wilkinson, D.G., Bhatt, S., and McMahon, A.P. (1989). Expression pattern of the FGF-related proto-oncogene int-2 suggests multiple roles in fetal development. Development *105*, 131–136.

Winnier, G., Blessing, M., Labosky, P.A., and Hogan, B.L. (1995). Bone morphogenetic protein-4 is required for mesoderm formation and patterning in the mouse. Genes Dev. *9*, 2105–2116.

Yamamoto, M., Meno, C., Sakai, Y., Shiratori, H., Mochida, K., Ikawa, Y., Saijoh, Y., and Hamada, H. (2001). The transcription factor FoxH1 (FAST) mediates Nodal signalling during anterior-posterior patterning and node formation in the mouse. Genes Dev. *15*, 1242–1256.

Zhou, X., Sasaki, H., Lowe, L., Hogan, B.L., and Kuehn, M.R. (1993). Nodal is a novel TGF-beta-like gene expressed in the mouse node during gastrulation. Nature *361*, 543–547.

Zorn, A.M., Butler, K., and Gurdon, J.B. (1999). Anterior endomesoderm specification in Xenopus by Wnt/beta-catenin and TGF-beta signalling pathways. Dev. Biol. *209*, 282–297.